Performance of FRP strengthened full-scale simply-supported circular hollow steel members under monotonic and large-displacement cyclic loading

T. Tafsirojjaman [a,b*], Sabrina Fawzia [a], David P Thambiratnam [a], Nicholas Wirth [a]

[a] School of Civil and Environmental Engineering, Faculty of Science and Engineering, Queensland University of Technology, 2 George Street, Brisbane, QLD 4000, Australia.

[b] Centre for Future Materials (CFM), School of Civil Engineering and Surveying, University of Southern Queensland, Toowoomba, QLD, 4350, Australia.

(*Corresponding author: tafsirojjaman@usq.edu.au, Tel: 61746315553)

Email addresses: tafsirojjaman@usq.edu.au (T. Tafsirojjaman),

sabrina.fawzia@qut.edu.au (Sabrina Fawzia), d.thambiratnam@qut.edu.au(DP Thambiratnam), n.wirth@connect.qut.edu.au (Nicholas Wirth)

Abstract

Steel structures are becoming more common in engineering construction as steel possesses excellent ductility, but steel members are often vulnerable to buckling, especially under seismic or cyclic loading. Hollow structural sections (HSS) often buckle locally under loading due to their thin steel walls and the need for rehabilitation and strengthening is increasing. In the present study, circular hollow section (CHS) steel members have been strengthened with both carbon fibre reinforced polymer (CFRP) and glass fibre reinforced polymer (GFRP). Their structural performance, along with that of their bare counterparts, is investigated subjected to monotonic and quasi-static large-displacement cyclic loading experimentally. The types of FRP reinforcement (CFRP and GFRP) and the loading condition (monotonic and cyclic) are

chosen as two main parameters in the test program. Results reveal the significant structural improvements of the strengthened CHS members under monotonic and cyclic loading. The ultimate moment capacities of the beams under monotonic and cyclic loading are enhanced by 51.0% and 35.4% respectively with CRFP strengthening and 43.3% and 31.5% respectively with GFRP strengthening compared to the bare beam. In addition, all the FRP strengthened specimens achieved higher moment capacities, rotational capacities, stiffness, energy dissipation capacities and ductility in comparison to their bare counterparts. Moreover, there is a good agreement found between the experimental and theoretically predicted ultimate moment capacities of the bare and strengthened CHSs with a mean ratio of 1.04 and a COV of 0.05.

Keywords

Circular Hollow Section (CHS) Steel members; Carbon fibre reinforced polymer (CFRP); Glass fibre reinforced polymer (GFRP); Strengthening; Monotonic loading; Cyclic loading; Theoretical prediction.

1. Introduction

Earthquake is a devastating natural disaster that can cause loss of lives and property. Structures in high seismic activity regions are subjected to cyclic loading. The vibrations due to earthquakes are expected to be much more extensive for taller buildings [1]. This is a significant concern for steel-framed structures as they tend to be much taller and have a higher population density. Human fatalities are common during earthquake events, due to partial or complete collapse of structures as the seismic loads can easily exceed the design capacity of structural elements. Structural failures during earthquakes have resulted in over 1.87 million deaths in the 20th century and during the period 1990-2010, an average of 2052 casualties occurred per event [2]. These seismic events have been occurring more frequently in recent years [3]. The necessity to mitigate the effects of earthquakes on all structures is rising due to this increase in

seismic activity. Steel framed structures in seismic regions are vulnerable to fracture failures, and there is the need for additional investigations in this area [4,5]. Increased and varied loads experienced during earthquakes can cause connections and single structural elements to exceed their design limits, causing failure in isolated sections of a structure or collapse of entire buildings [6]. Earthquake loads affect both onshore and offshore structures, while additional wave effects must be considered for offshore structures [5].

The application of CHS steel members has been increasing significantly to build different offshore and onshore structures. In offshore structures, CHS is significantly used to build jacket structures which are sometimes subjected to bending and cyclic loading due to wave forces [5]. Moreover, the bending behaviour of CHS members is also important to investigate as CHS columns are subjected to bending when loaded eccentrically. Though structures are currently designed with a greater focus on earthquake forces, many existing buildings remain vulnerable. The 2010 earthquake in Christchurch, New Zealand, was followed by surveys that revealed many structures in the area might be structurally insufficient to withstand seismic events [7]. This earthquake with a magnitude of 7.1 in September of 2010 was followed by a magnitude 6.3 earthquake five months later. The first earthquake and subsequent aftershock caused roughly 15 billion U.S. dollars in structural damage and 185 casualties [7]. Many steel structures, including various healthcare services, suffered significant damage during the 1994 earthquake in Northridge. Damages were seen in low and high-rise steel buildings, both new and old. Therefore, strengthening the CHS steel members of buildings is extremely important for improved performance and safety in regions of seismic activity. Effects of service load increments over the structure's life cycle, reduction of steel material properties over time, or the inadequate design of structural members are also reasons to consider strengthening in addition to seismic loading. Research on the rehabilitation and strengthening of structural steel sections is hence needed to address these concerns.

Fiber reinforced polymer (FRP) is continually growing in popularity as a strengthening material due to its advantageous properties such as high tensile strength, the very high strength-to-weight ratio [8,9], better flexibility [10] and excellent corrosion resistance [11] etc.

It can however be vulnerable to fires which are common in seismic events. Bhatt et al. [12] concluded that CFRP strengthened RC beams insulated with fireproofing spray of 19 to 32 mm thick can withstand service load levels for four hours under an ASTM E119 [13] standard fire exposure. Moreover, the minimum fire resistance level requirement for an FRP strengthened square hollow column can be achieved using a proper insulation system [14]. Hence, a proper insulation system is an important matter that needs to be explored through significant research work, to enable a suitable option to protect FRP strengthened members under expected fire during a seismic event. CFRP strengthened CHS has been shown to have improved structural performance such as higher stiffness [15], greater load capacity [16], greater ultimate bending strength [17], higher ductility [17], delayed local bucking [18] and energy dissipation capacity [17,19] compared to its bare counterpart. This improvement of structural performance was found to increase as the number of CFRP sheets increased [15,19]. Numerical analyses and experimental tests showed similar improvements in structural performance. Increases in load capacity, fatigue life and deflection at failure were also seen in CFRP strengthened concrete beams under cyclic loading [20]. Similar improvements in structural performance have been seen in the universal beam (UB) elements. Additionally, the stiffness, deflection and fatigue life improvements were found in the CFRP wrapped UB [21]. Steel frames have shown less tip displacement when strengthened with CFRP [22,23]. Moreover, CFRP also has shown its effectiveness in enhancing the impact resistance capacity of steel members [24,25].

GFRP has also been shown to improve the structural performance of various steel sections in existing studies. It has been shown to increase the ultimate bending strength of concrete-filled CHS. These strengthened members had higher stiffness than bare members, which may have

caused the reduction in energy dissipation seen [26]. Additionally, GFRP has been used to improve the structural response of other steel sections. The ultimate load capacities and ultimate bending strengths of GFRP wrapped RHS and UB steel sections increased over those of their bare counterparts [27–31]. Member stiffness was shown to increase due to GFRP strengthening in UB tests [30,31]. An increase in energy dissipation, ductility and fatigue life was also seen due to GFRP wrapping [28,30,31]. Ductility and energy dissipation were shown to increase in cyclic load cases [32]. Moreover, both CFRP and GFRP strengthening have been shown to be effective for enhancing the flexural performance of reinforced concrete beams [33] as well as pre-cracked reinforced concrete beams [34]. As previous studies on FRP show significant improvements in structural performance, the use of both CFRP and GFRP are promising options for the reinforcement of steel sections.

Hence, CFRP and GFRP strengthening techniques can be effective methods to mitigate the vulnerability of CHS steel members under seismic or cyclic loading. However, the cyclic bending behaviour of CFRP and GFRP strengthened CHS members under simply supported conditions has yet to be studied extensively to fill the lack of research knowledge in this area. This paper investigates the effects of CFRP and GFRP strengthening to enhance the structural performance of simply supported CHS beams under monotonic and large-displacement cyclic loading. The load is applied at the centre of each beam by a hydraulic actuator. Bare, CFRP and GFRP strengthened CHS beams were prepared for monotonic and cyclic loading tests, totalling six specimens. Each CHS member was near-identical in length, outside diameter and wall thickness and the same adhesive was used in all the specimens. The structural performances of the bare, CFRP and GFRP strengthened specimens with respect to ultimate moment capacity, moment capacity degradation, secant stiffness, energy dissipation, and ductility under monotonic and cyclic loading are compared. Moreover, the ultimate moment capacity of bare and FRP strengthened beams under monotonic and cyclic loading have been

theoretically predicted and compared with the corresponding experimental results. In addition, based on the information from the present study, appropriate cyclic design factors have been recommended that can be used in designs. The research outcomes can be useful to restore the structural integrity of CHS members in earthquake-prone areas through FRP strengthening.

2. Experimental Program

2.1 Materials

The experimental test specimens were prepared using steel CHS members, CFRP, GFRP and epoxy adhesive. OneSteel Limited, Australia, supplied the CHS steel members. Test specimens were cut to identical lengths. Each specimen was 1300 mm overall length, 1150 mm span, with an outside diameter of 76.1 mm and a wall thickness of 2.3 mm. Steel coupons were formed from the CHS section according to AS1391 standards [35] to measure the mechanical properties of steel. The average yield stress of the steel was 380 MPa, tensile strength was 475 MPa and the elastic modulus was 190 GPa. The CFRP used was supplied by BASF construction chemicals Australia Pty Ltd. The used CFRP was normal modulus CF130, $300g/m^2$, 0.176 mm nominal thickness, and unidirectional. CG Composites Australia Pty Ltd supplied the unidirectional GFRP sheets. Unidirectional CFRP and GFRP sheets were chosen based on their excellent tensile properties which can be very useful for enhancing the flexural performance of the beam by contributing tensile strength along the beam in the tensile zones. The properties for CFRP and GFRP were obtained from tensile coupon tests, conducted according to ASTM:D3039-08 [36] by one of the authors. The obtained elastic modulus and tensile strength for CFRP were 75 GPa and 987 MPa, respectively [26] and for GFRP were 55 GPa and 1065 MPa, respectively [16]. The measured average thickness of the CFRP and GFRP laminates were 0.60 mm and 0.65 mm respectively. MBrace saturant epoxy was used as an adhesive for the FRP strengthening. BASF construction chemicals Australia Pty Ltd supplied

the two-part adhesive used. The MBrace 3500 primer was used to promote adhesion between the FRP and steel as a base layer, with MBrace 4500 epoxy used directly on top and between FRP layers. The mechanical properties of adhesive were obtained by tensile coupon tests in accordance with ASTM: D638-10 [37] by one of the authors. The obtained elastic modulus and tensile strength of adhesive were 2.86 GPa and 46 MPa, respectively [16]. Moreover, the mechanical properties of materials are summarised in Table 1.

Table 1: Mechanical properties of materials.

Materials	Elastic Modulus (GPa)	Tensile Strength (MPa)	Thickness (mm)
CHS Beam	190	475	2.3
CFRP	75	987	0.60
GFRP	55	1065	0.65
MBrace Adhesive	2.86	46	-

2.2 Experimental Specimens and Strengthening Schemes

A total of 6 specimens were prepared – one bare steel CHS, CFRP and GFRP strengthened CHS each for monotonic and cyclic loading tests. Each specimen was labelled for precise identification of its preparation and loading conditions. The first part of the identifier (BB) or (SB) specifies whether the beam is bare or strengthened respectively. Next pertains to strengthening material – (B) for the bare beam, (C) for CFRP strengthening and (G) for GFRP strengthening. The last term specifies whether the loading is monotonic (M) or cyclic (C). Details for each specimen are given in Table 2.

Table 2: Experimental specimens matrix.

Specimen types	Specimen identifier	Types of FRP	Loading condition
Bare beam	BB-B-M	-	Monotonic
Strengthened beam	SB-C-M	CFRP	Monotonic
Strengthened beam	SB-G-M	GFRP	Monotonic
Bare beam	BB-B-C	-	Cyclic
Strengthened beam	SB-C-C	CFRP	Cyclic
Strengthened beam	SB-G-C	GFRP	Cyclic

Both CFRP and GFRP sheets were applied using the same dimensions, layout and orientation. All specimens were strengthened with three layers of FRP as results from previous studies showed that strengthening the CHS with three layers of CFRP is most effective under monotonic [15] and cyclic loading [19]. Moreover, previous studies concluded that any further extension of the wrapping length after a certain bond length had little or no effect on the performance of CHS members under monotonic [15] and cyclic loading [19]. The bond length is considered from loading points to the wrapping ends towards the support and the sufficient bond length has been chosen as 300 mm in the present study based on available literature [15,16,19]. Hence, the FRP layers were 600 mm long and applied at the centre of the CHS member, with 300 mm of the sheet on either side of the steel section's centreline. The first and second layers were laid with their fibre directions running longitudinally (L) along the CHS length. The third layer was placed laterally so that its fibre direction was perpendicular to the beam's length in a hoop (H) layout to confine the first two layers for better debonding resistance. A schematic diagram for the FRP pattern is provided in Figure 1.
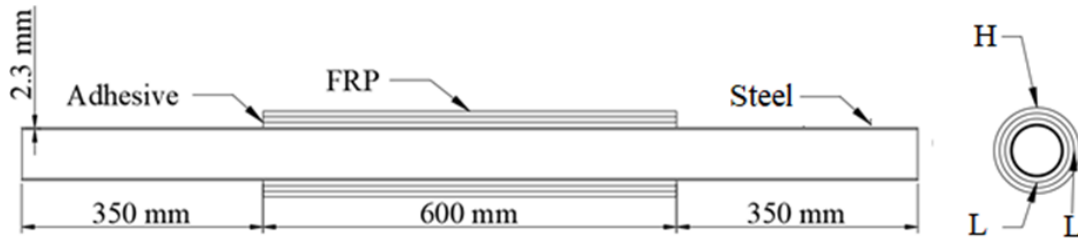
Figure 1: Schematic diagram pattern for FRP strengthened CHS beams.

2.3 Specimen Preparation and Strengthening Process

Preparation of the test specimens for wrapping is an essential step to ensure a quality bond between FRP and steel. The entire outside portion of the CHS was sandblasted to achieve a clean and rough surface and free of any impurities. This was done as previous reports have found sandblasting to be an effective method of preparing steel surfaces for FRP bonding [38,39]. Acetone was then used to clean any remaining impurities from the surface of the steel. First, the two-part MBrace 3500 primer was mixed and applied to the specimens. The adhesive primer has been shown to increase member strength of CFRP strengthened members over that of CFRP strengthened members without the primer [16]. The two-part MBrace 4500 saturant was mixed according to manufacturer guidelines and applied to the primer-coated surface of the beams. Precut FRP sheets were applied on top of the adhesive and wrapped around the member. These sheets were then rib-rolled to ensure fibres were fully saturated, creating a consistent thickness and completely laminating sheets. Additional layers of FRP were applied after recoating with MBrace 4500 saturant and rib-rolled as was done for the first layer. Once FRP layering was completed, the specimen was covered with masking tape to prevent premature debonding while curing. Each specimen was then placed carefully so that FRP was not touching anything and left to cure for 24 hours. After the initial 24-hours curing period, the masking tape was removed. The exposed FRP was then left to fully cure for a minimum of 14 days before testing. Completed specimens ready for testing can be seen in Figure 2.
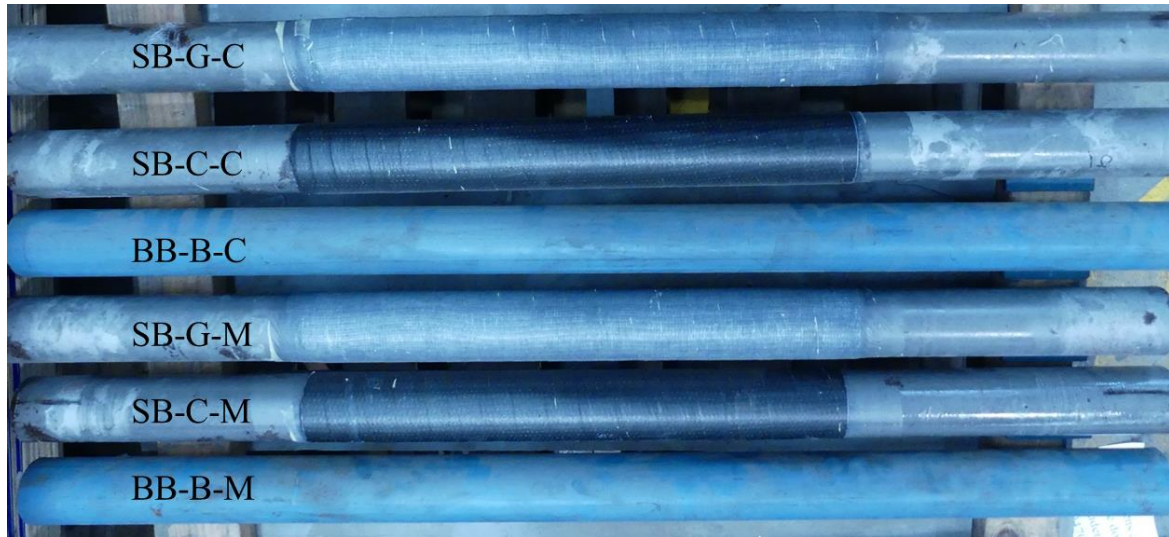
Figure 2: Prepared specimens for the experiment.

2.4 Experimental Setup and Loading Protocol

The CHS beam was placed horizontally on supports at 75 mm from each end of the beam, creating an 1150 mm span. Supports at both ends were simply supported pinned connections designed to allow rotation. The supports used a round bar below the specimen for the vertical support on the monotonic push load test. An additional plate with a round bar (mirroring the support below the beam) was bolted to the support above the specimen at each end for the cyclic load tests to provide vertical support on the pull cycle. A bar was welded vertically on either side of the beam at the supports to ensure the specimen would not move laterally. The hydraulic actuator applied its load to the centre of the beam while the end supports provided vertical restraint, forming a three-point loading setup. This hydraulic load was applied through a round bar above the beam for the monotonic load case, with an additional round bar bolted to the hydraulic below the beam for the reverse cycle of the cyclic load case. To reduce the possibility of crashing due to the concentrated load from the round bar, a thick plate was placed between the specimen and round bars connected to the hydraulic. A schematic diagram of this setup can be seen in Figure 3, and a photograph of the setup in Figure 4.
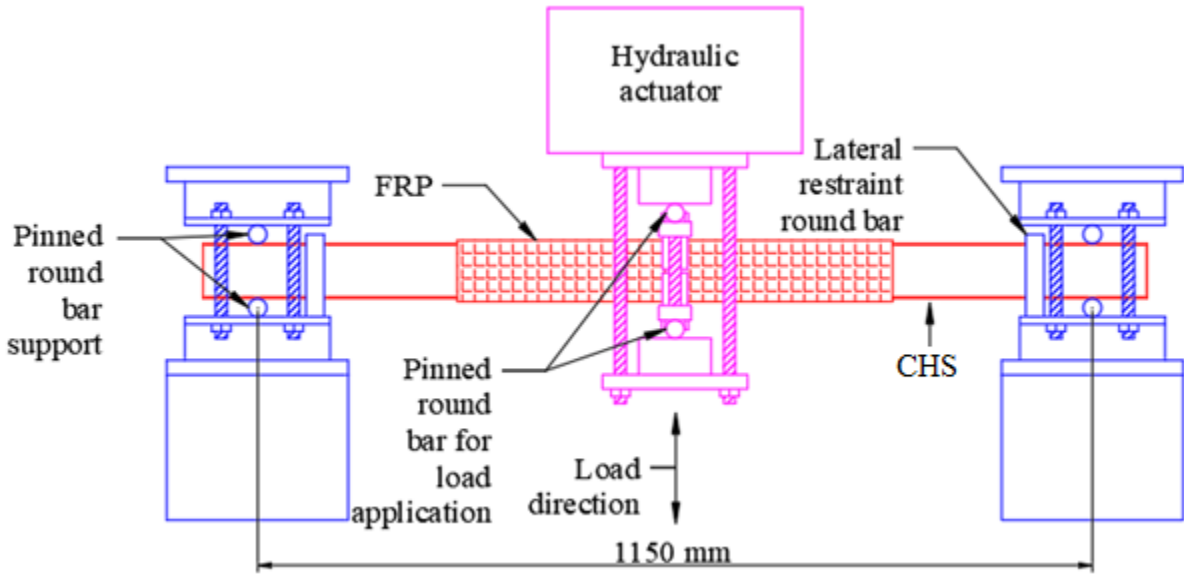
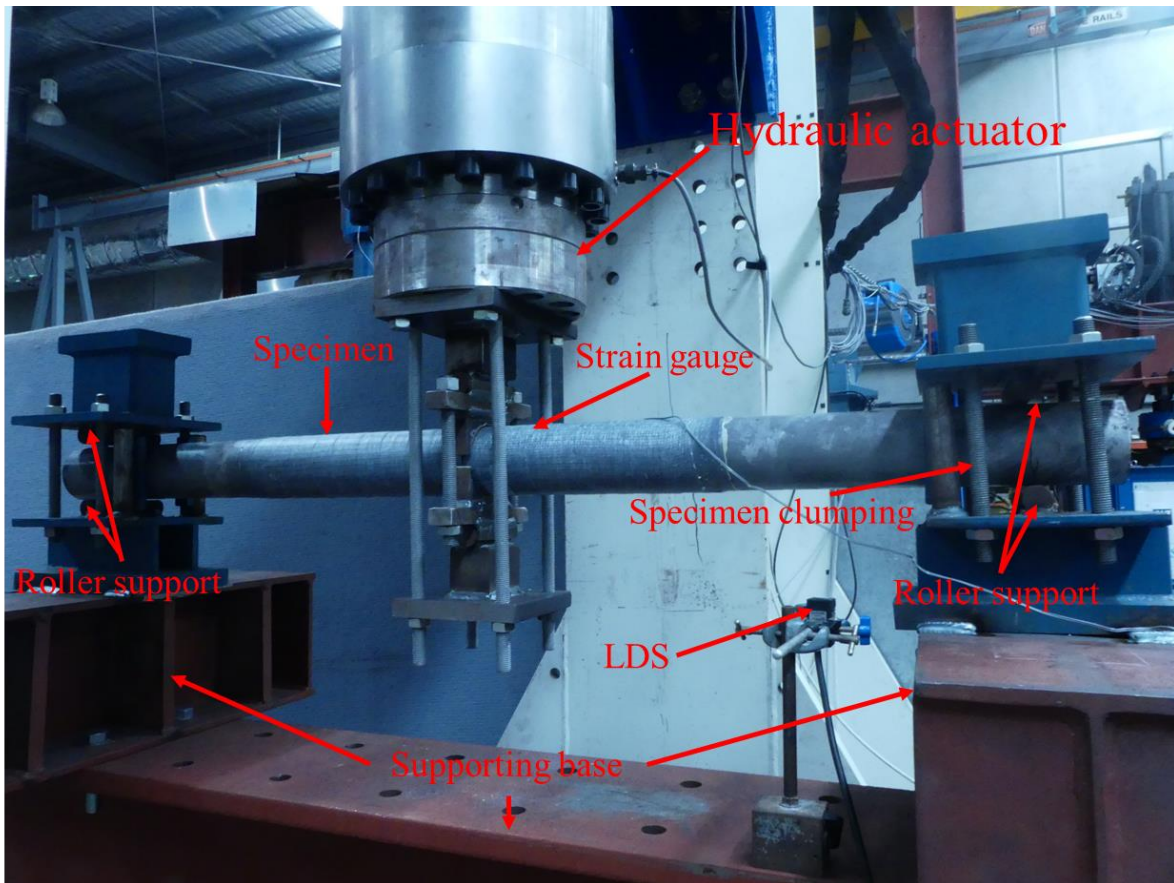Figure 3: Schematic diagram of the experimental setup.

Figure 4: Photograph of the experimental setup.

The loading protocol engaged a hydraulic machine that is able to apply up to 1000 kN in both monotonic and cyclic conditions. The machine measured the load applied and its corresponding displacement. The displacement near the support of the beam was measured by a laser displacement sensor (LDS). Cyclic load tests were applied at a quasi-static loading rate (12.5mm/min) by increasing the displacement of subsequent cycles to simulate a far-field earthquake as required in ANSI/AISC 341-16 [4] and shown in Figure 5. The failure phenomenon of the tested bare, CFRP and GFRP strengthened CHS members are shown in Figure 6.
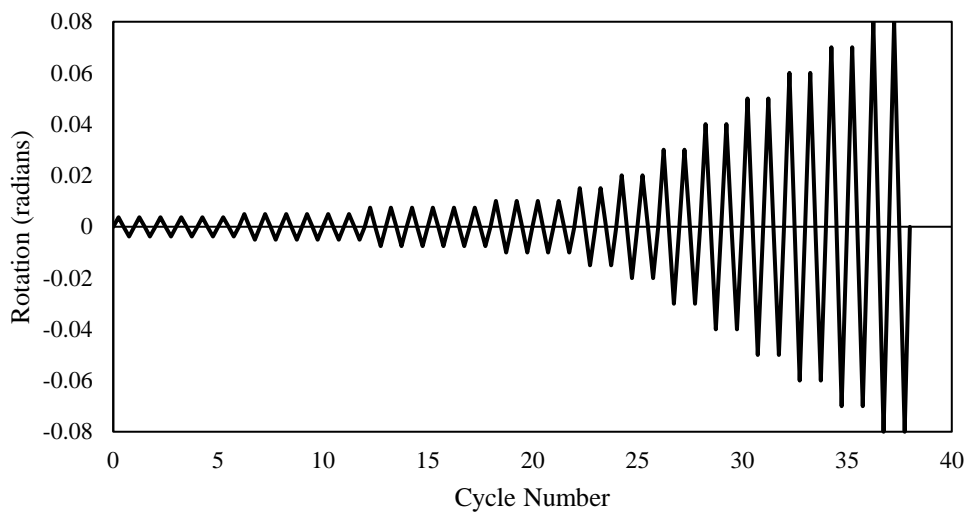

Figure 5: Cyclic loading protocol (adapted from [4]).

Figure 6: Tested bare, CFRP and GFRP strengthened CHS members.

3. Experimental Results and Discussions

The structural response of CHS beams is improved by the strengthening characteristics of CFRP and GFRP. Longitudinal fibres of the FRP sheets were aligned with the direction of the beam and locked in place with a transversely orientated hooping layer, which resulted in the beams having improved ultimate moment capacity, energy dissipation capacity, secant stiffness and ductility.

3.1 Behaviour under monotonic loading

Moment-displacement curves are used to display the response of bare, CFRP and GFRP strengthened beams under monotonic loading. The moment capacity was calculated using the formula for a simply supported beam with a point load at mid-span (*PL/4*), where *P* is the applied load derived from the experiment and L is the span length (1.15 m). The bending response of the three beams under monotonic loading has been plotted in moment-rotation curves as shown in Figure 7. This graph shows both FRP strengthened beams have a significant increase in moment capacity over the bare steel beam. The ultimate moment capacities of the

beams under monotonic loading show increases of 51.0% with CRFP strengthening (8.0 kN.m) and 43.3% with GFRP strengthening (7.6 kN.m) compared to the bare beam (5.3 kN.m). Additionally, both strengthened beams reached higher rotations at their ultimate capacities and showed less buckling under monotonic loading than the bare beam. The rotations reached were 0.034 radians, 0.044 radians and 0.059 radians for bare, CFRP strengthened and GRRP strengthened CHS beams, respectively. Therefore, the strengthening techniques of both CFRP and GFRP can effectively improve the structural performance of CHS beams under monotonic loading. A 5.4% higher increase in the ultimate moment capacity is noted in the CFRP strengthened beam compared to the GFRP strengthened beam. But, the GFRP strengthened beam shows 34.1% higher rotational capacity before reaching the ultimate moment capacity over that of the CFRP strengthened beam. Moreover, all the bare and strengthened members displayed typical ductile modes of failure as shown in Figure 6. Local buckling in the compression zone at the middle of the specimen was the prominent failure mode for all the bare and strengthened members. Debonding and crushing of the FRP composites in the compression zone at the middle of the specimens were noticed for both CFRP and GFRP strengthened members as well. The CFRP and GFRP composites in the tension face and at end of wrapping remained intact. It may be due to the application of sufficient bond length of FRP composites.
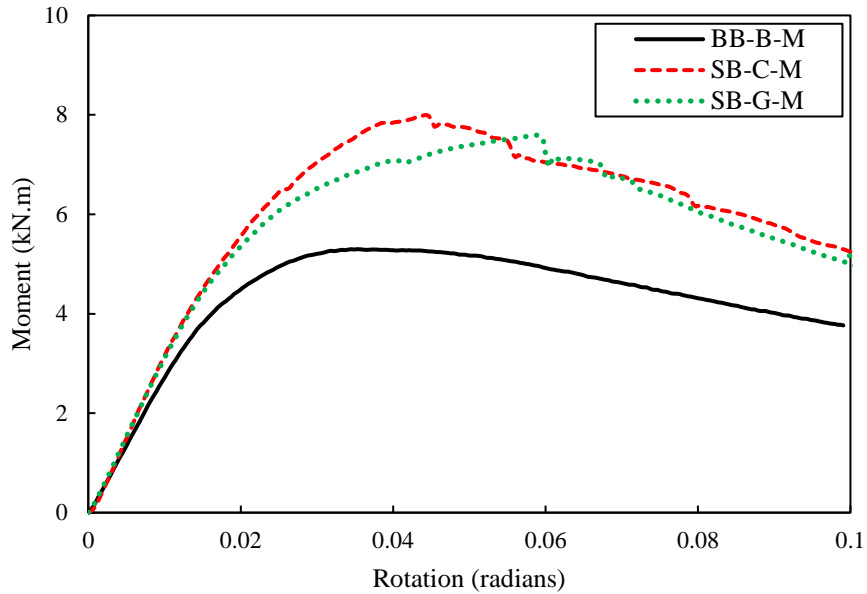
Figure 7: Moment-displacement curves of bare, CFRP and GFRP strengthened beams under

monotonic loading.

The applied load was divided by the corresponding displacement to obtain the secant stiffness, which was then plotted against the rotation. Figure 8 compares the secant stiffness for each of the three specimen types tested under monotonic loading. An increase in maximum stiffness of 15.1% for CFRP strengthening and 13.7% for GFRP strengthening can be seen, resulting in a maximum secant stiffness of 1912.2 kN/m and 1889.5 kN/m for the CFRP and GFRP strengthened CHSs, respectively, over the bare CHS maximum stiffness of 1661.4 kN/m. The secant stiffness starts to reduce with the increase in rotation for each of the three types of the beam after reaching its maximum secant stiffness. While the maximum secant stiffness of FRP strengthened beams was not significantly higher than that of the bare beam, their stiffness was much higher than the bare beam at the ultimate rotation. At the ultimate rotation, secant stiffness increases of 45.4% and 38.5% were observed for the CFRP and GFRP strengthened CHSs respectively. Hence, both CFRP and GFRP strengthened steel members have a greater stiffness than their bare counterparts. But the CFRP strengthened CHS member shows slightly

higher (5.0%) secant stiffness than the GFRP strengthened CHS member as the stiffness property of the CFRP sheet is slightly higher than the GFRP sheet.
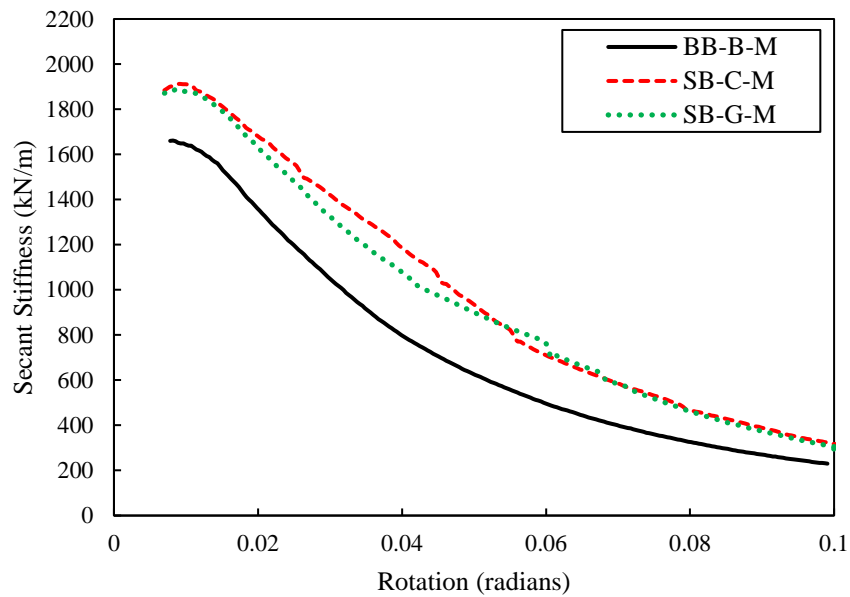

Figure 8: Secant stiffness-displacement curves of the bare, CFRP and GFRP strengthened beams under monotonic loading.

Finally, the effect on the ductility factor of each beam was considered. The ductility of a beam greatly affects the response of a steel-framed structure under seismic loading. The ratio of dissipated energy at the ultimate load to dissipated energy at the yield point is used to determine the ductility factor of the beam [40]. The yield point was found by using the general yield moment method [41]. Figure 9 displays the ductility factors for all beams. Both FRP strengthened beams clearly show higher ductility over the bare steel beam. The ductility factor of bare steel CHS is 1.88, while those for the CFRP strengthened CHS beam is 1.95 and GFRP strengthened CHS beam is 2.73. These results show that the CHS beam's ductility has increased by 3.6% and 44.7% due to CFRP and GFRP strengthening, respectively. Moreover, the GFRP strengthened beam has shown 39.7% higher ductility compared to the CFRP strengthened beam

due to its higher rotational capacity at the ultimate moment and less moment degradation after the ultimate moment capacity.
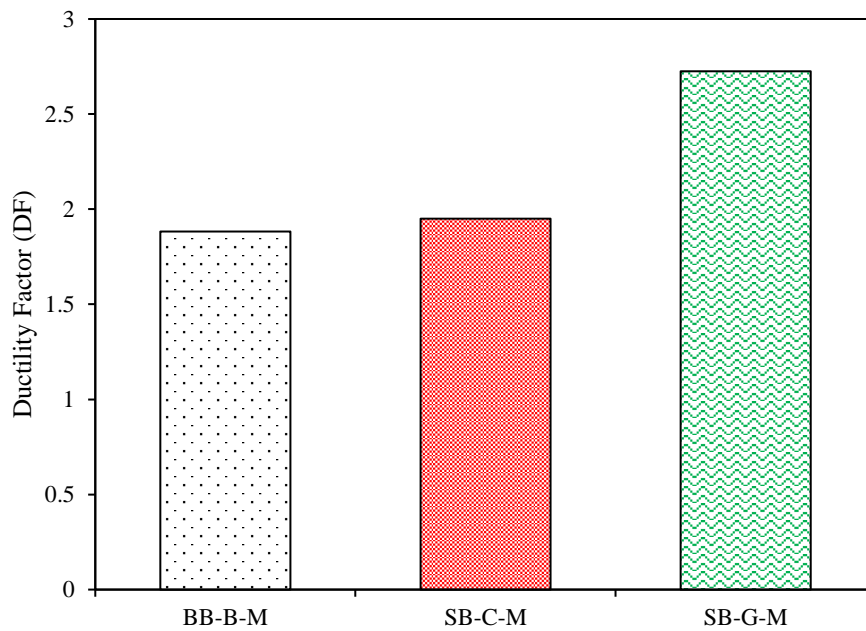

Figure 9: Ductility factors of the bare, CFRP and GFRP strengthened beams under monotonic loading.

3.2 Behaviour under cyclic loading

The behaviour of CFRP and GFRP strengthened CHS members under cyclic loading were evaluated and compared with the bare CHS member to investigate the effectiveness of CFRP and GFRP strengthening techniques. To simulate loading effects during an earthquake, each specimen was tested under quasi-static cyclic loading. The cyclic hysteretic response, moment capacity backbone curve, secant stiffness and energy dissipation capacity were plotted and compared for each member. The CFRP and GFRP strengthening techniques are very effective as seen in these results.

3.2.1 Experimental hysteretic behaviour

The moment-rotation hysteretic analysis was used to assess the cyclic bending response of bare and FRP strengthened CHS steel members. The bare, CFRP and GFRP strengthened CHS members' moment-rotation hysteretic responses are displayed in Figure 10(a), Figure 10(b) and Figure 10(c), respectively. It can be seen from these figures that all the bare, CRFP and GFRP strengthened CHS members have exhibited inelastic responses. Additionally, the graphs show flat portions at zero loads for each cycle, where displacements increased while the loads did not. These flat sections are due to the permanent deformations of the beams at the supports where unrestrained rotations occurred. After the yielding, all the members show a reduction of moment capacity in the second rotational cycle compared to the first rotational cycle for each rotational level. Moreover, increasing the rotational level resulted in a further reduction of moment capacity as well. Under cyclic loading, the CFRP and GFRP strengthened CHS members had significantly higher moment capacity when compared to the bare CHS member. In the positive rotation, the ultimate moment capacity for the bare CHS was 5.14 kN.m, while that for the CFRP and GFRP strengthened CHSs were 6.96 kN.m and 6.43 kN.m respectively. This is a 35.4% increase for CFRP strengthening and a 31.5% increase for GFRP strengthening. Additionally, increases in ultimate moment capacity were seen in the negative rotation cycles for both CFRP and GFRP strengthening as well. The ultimate moment capacity in the negative direction was 5.07 kN.m for the bare, 6.43 kN.m for the CFRP strengthened and 6.53 kN.m for GFRP strengthened CHS members. This clearly shows an increase in the ultimate moment capacity of 26.8% for the CFRP and 28.8% for GFRP strengthened members over the bare member in the negative rotation. Hence, the positive rotation has a greater ultimate moment capacity over the negative rotation for each specimen type. Moreover, both the positive and negative rotational level at ultimate moment capacity for each beam type was 0.03 radians, 0.03 radians and 0.04 radians for bare, CFRP and GFRP strengthened CHS. Therefore, the

CFRP strengthened CHS beam achieved a higher ultimate moment capacity due to CFRPs material property of high stiffness. But, the GFRP strengthened CHS beam achieved a higher rotation level than that of the bare and CFRP strengthened CHS members due to its increased ductility. Moreover, local buckling, debonding and crushing of the FRP composites were noticed in both of top and bottom faces at the middle of all specimens due to the push-pull loading applied during cyclic tests as shown in Figure 6. No debonding at the end of the FRP composites was noticed.
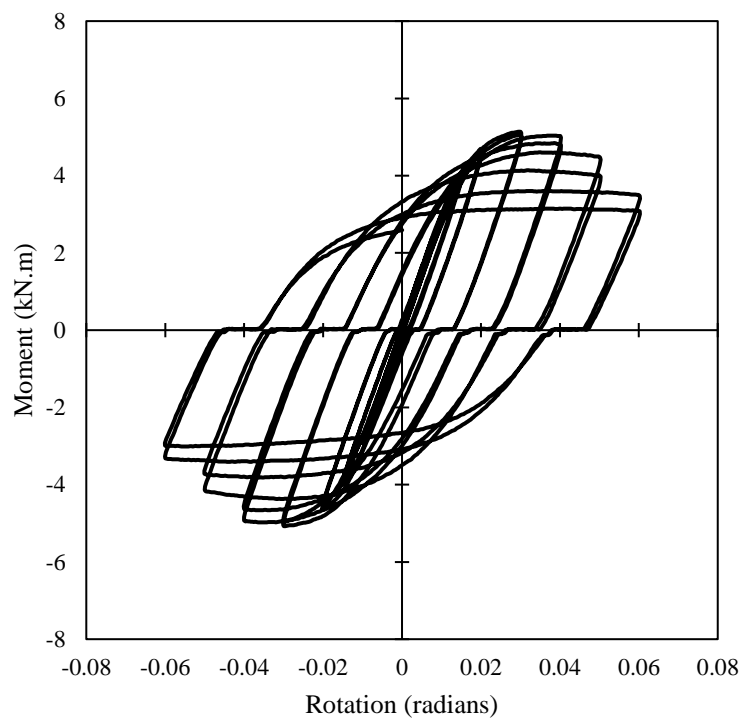
(a)
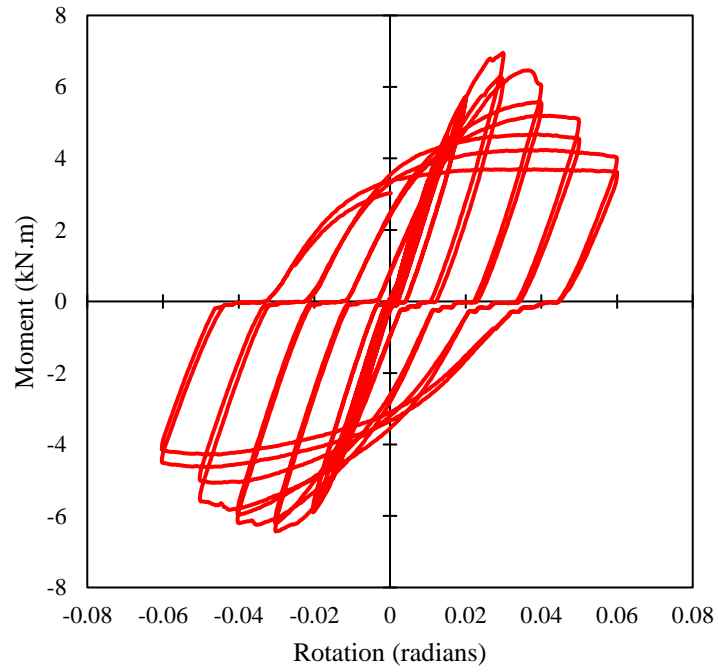
(b)
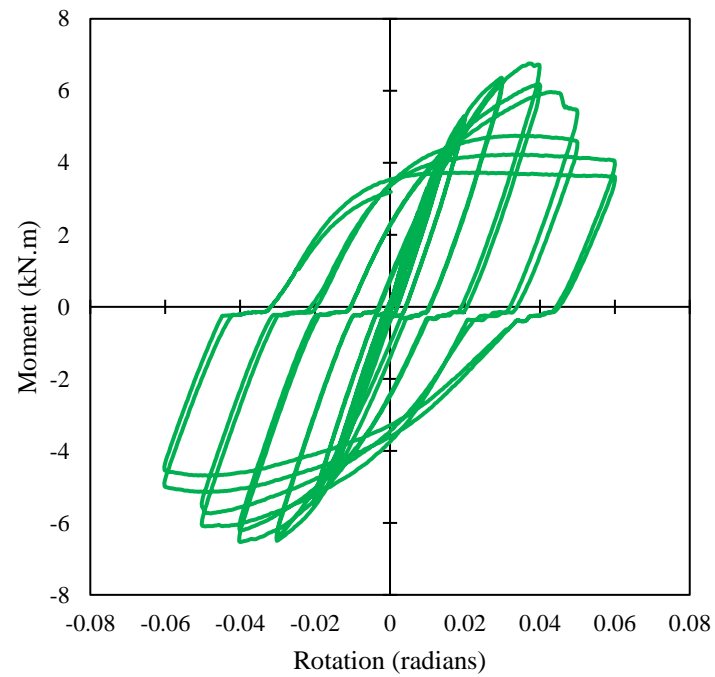
(c)

Figure 10: Moment capacity-rotation hysteresis curves of the (a) bare, (b) CFRP and (c)

GFRP strengthened CHS beams.

3.2.1 Moment Capacity Degradation Behaviour

Moment capacity backbone curves of the moment-rotation hysteresis responses were developed for each specimen to analyse their moment capacity degradation. The moment at maximum rotation for the first cycle of a rotation level was plotted against each rotational level to create the backbone curves. The moment-rotation backbone curves of cyclically loaded bare, CFRP and GFRP strengthened CHS beams are plotted in Figure 11. This makes an additional comparison of the data shown in Figure 10(a), Figure 10(b) and Figure 10(c). All three beams behaved stably in the negative and positive rotations and achieved the symmetrical response for moment-rotation. After reaching the ultimate moment capacity, the moment capacity for each beam type decreased with the increased rotational cycle. The reduction in the moment capacity of each specimen is the result of local buckling in the beams. A greater moment capacity was achieved by both CFRP and GFRP strengthened members compared to their bare counterparts. The maximum moment capacity of the bare beam in the positive direction was 5.13 kN.m at a rotation of 0.03 radians, while at 0.06 radians, the moment capacity had reduced to 3.48 kN.m. The maximum moment capacity for the CFRP strengthened CHS at 0.03 radians was 6.92 kN.m, reducing to 4.04 kN.m at 0.06 radians, while the maximum moment capacity at 0.04 radians for the GFRP strengthened CHS was 6.42 kN.m, reducing at 0.06 radians to 4.07 kN.m. This shows at the maximum rotation of 0.06 radians, both CFRP and GFRP strengthened beams had increased moment capacities of 16.3% and 17.2%, respectively, compared to the bare steel CHS beam. The structural behaviours in the negative rotation for all beam types tested were almost identical to their performance in the positive rotation.
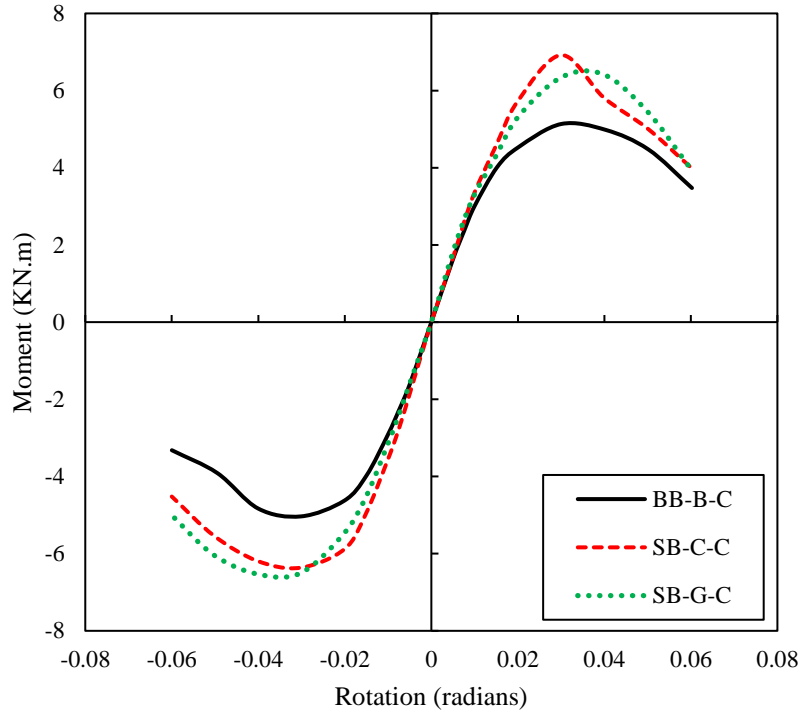
Figure 11: Moment capacity-rotation hysteresis backbone curves of the bare, CFRP and

GFRP strengthened CHS beams.

3.2.2 Secant Stiffness

The load applied at maximum displacement for each rotation level was divided by the

maximum displacement for that rotation level to calculate the secant stiffness for each beam.

The secant stiffness for the bare, CFRP and GFRP strengthened CHS beams were plotted

against the rotation level for that secant stiffness and shown in Figure 12. All three beams had

reduced secant stiffness as the loading and rotation levels increased. The maximum secant

stiffness in the positive rotation was 1817.7 kN/m for the bare CHS, 2029.9 kN/m for the CFRP

strengthened CHS and 1998.2 kN/m for the GFRP strengthened CHS at a rotation of 0.01

radian. This shows an increase in secant stiffness of 11.7% and 9.9%, respectively, for the

CFRP and GFRP strengthened beams over the bare beam. The degradation of the stiffness of

bare CHS was slightly more compared to the strengthened beams, although all reduced in

stiffness gradually. At the rotational level of 0.06 radians, the stiffnesses of CFRP and GFRP strengthened CHS beams were 17.4% and 19.1% higher than the stiffness of the bare CHS beam. Hence, the GFRP strengthened beam experienced slightly less stiffness degradation (2.3%) in comparison to the CFRP strengthened beam. Therefore, both FRP strengthening techniques are seen to be very useful in increasing stiffness when used on CHS steel beams. The greater stiffness properties of the CFRP resulted in a slightly higher stiffness (1.6%) for the CFRP strengthened beam over the GFRP strengthened beam. An almost similar structural response was seen for the stiffness of all three test beam types in the negative rotation.
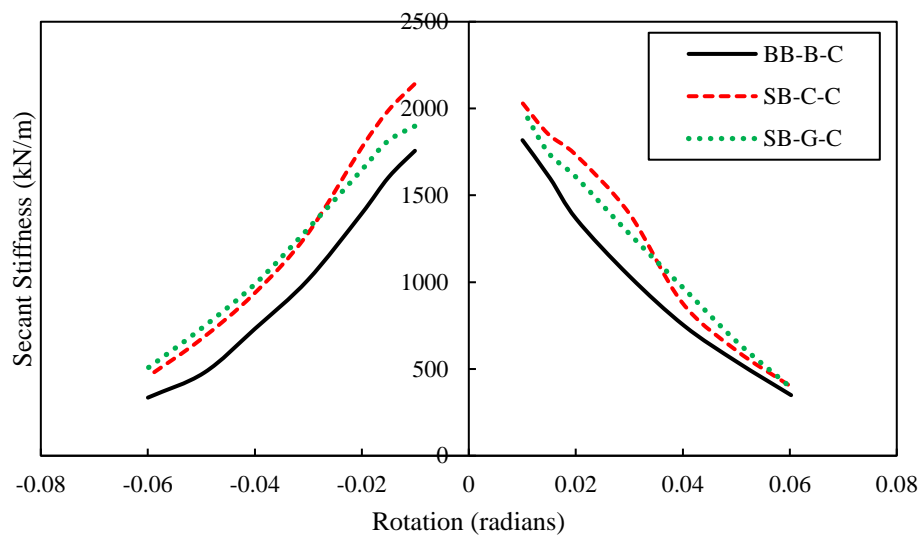

Figure 12 Secant stiffness-rotation curves of the bare, CFRP and GFRP strengthened CHS beams

3.2.3   Energy Dissipation Capacity

The effect of CFRP and GFRP strengthening on energy dissipation capacity under cyclic loading has been analysed. The inelastic deformation of key structural elements is the primary method of seismic energy dissipation. Steel framed buildings usually dissipate energy through inelastic deformation of beams, panels and column bases. Hence, the energy dissipation

capacity of bare, CFRP and GFRP strengthened CHS beams is a vital parameter for earthquake loading considerations. The total enclosed area by all cycles in each rotation level was plotted against that particular rotation to create the energy dissipation capacity curve for each specimen. Figure 13 shows the comparison of the energy dissipation capacities of all beam specimens. Within the elastic region (approximately the first 0.01 radians), the energy dissipated for all beams was low due to the high initial stiffness of all beams. Moreover, the energy dissipation capacities of the bare and strengthened beams were close till the rotational level of 0.04 radians although the moment capacities have bigger differences. This phenomenon was due to the lower enclosed areas of hysteresis loops of strengthened beams because of the high stiffness characteristics of strengthened beams compared to bare beam. However, as the beams yielded, the energy dissipation capacities of the CFRP and GFRP strengthened CHS beams increased at higher rates than the bare CHS beam due to less moment degradation of strengthened beams. The energy dissipated at the ultimate moment capacity for the bare beam was 1.9 kN.m, while that for the CFRP and GFRP were 2.2 kN.m and 2.3 kN.m, respectively. This is an increase of 14% for the CFRP strengthened and 19.2% for the GFRP strengthened CHS beam over the bare CHS beam. Hence, both FRP materials have been shown to increase the energy dissipation capacity of the CHS beams. The GFRP strengthened beam, however, had a 4.6% higher energy dissipation capacity than the CFRP strengthened beam due to its higher ductility properties.
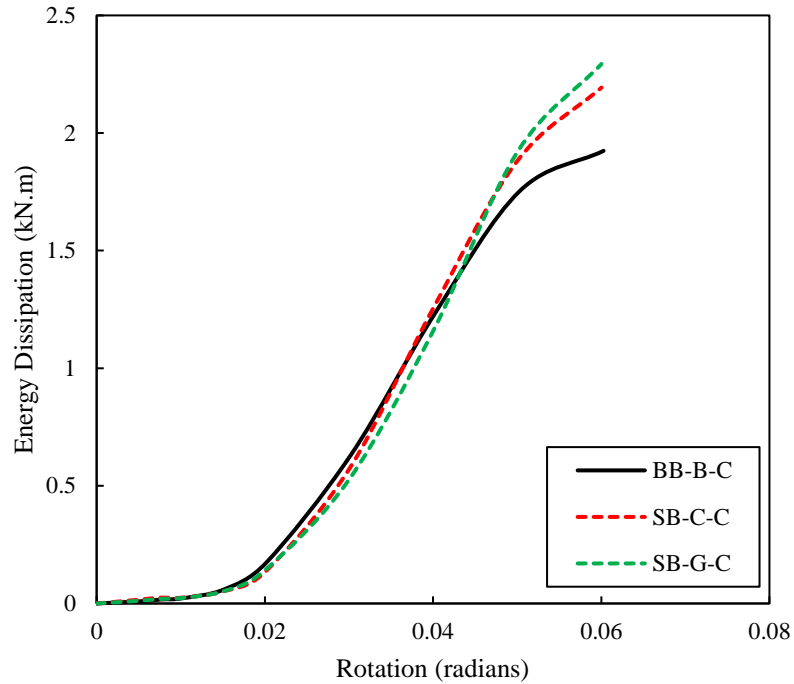
Figure 13: Energy dissipation-rotation curves of the bare, CFRP and GFRP strengthened

CHS beams.

4. Comparison between experimental and theoretically predicted ultimate moment capacities

The ultimate moment capacity of the bare and FRP strengthened beams under monotonic and as well as under cyclic loading has been theoretically predicted and compared with their experimental ultimate moment capacity. Plastic section moduli of CFRP and GFRP strengthened beams were calculated using the method outlined in Haedir et al. [42] though they proposed the method only for CFRP strengthened beams. The transformed section of FRP strengthened CHS according to Haedir et al. [42] to calculate the moment capacity of FRP strengthened CHS beam, is shown in Figure 14.
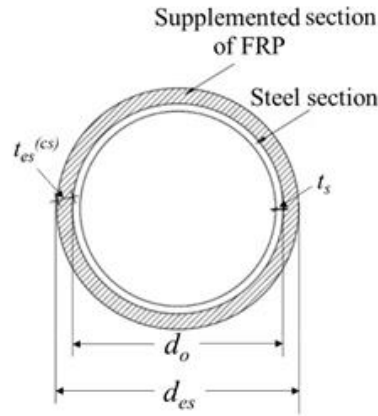
Figure 14: Transformed section of FRP strengthened CHS

The diameter of the transformed section of FRP strengthened CHS (d_{es}) can be expressed as below [42]:

$$d_{es} = d_o + 2t_{es}^{(CS)} \qquad\qquad \text{Equation 1}$$

where the outer diameter of the steel profile of FRP strengthened CHS is denoted by d_o and the thickness of the supplemented section of FRP to steel is denoted by $t_{es}^{(CS)}$ and specified by Haedir et al. [42].

The ultimate moment capacity of FRP strengthened CHS section (M_{es}) can be predicted by the following equation:

$$M_{es} = f_y Z_{ese} \qquad\qquad \text{Equation 2}$$

In the above equation, f_y refers to the yield strength of steel and Z_{ese} refers to the effective section modulus of the transformed section of FRP strengthened CHS which depends on the section classification, i.e. slender section non-compact section or compact section and specified by Haedir et al. [42].

Moreover, the ultimate moment capacity of the bare members under monotonic loading was predicted by following AS4100 [43]. The quasi-static effect for cyclic loading was used to estimate the beam's ultimate moment capacity under cyclic loading. This was calculated by

multiplying the predicted ultimate moment capacity under monotonic loading with the cyclic design factor. The cyclic design factor was taken as 0.97, 0.87 and 0.926 for the bare steel, CFRP strengthened and GFRP strengthened beams, respectively. These values are obtained as the ratios of the experimental maximum moment capacities under current cyclic loadings to those under monotonic loadings for the bare, CFRP strengthened and GFRP strengthened specimens respectively. The predicted experimental and theoretical ultimate moment capacities are compared in Table 3. The bare steel, CFRP and GFRP strengthened CHS experimental values for ultimate moment capacities are similar to those of the predicted theoretical values for the corresponding beams with a mean ratio of 1.04 and a COV of 0.05. Hence, this theoretical prediction model can be utilized for both CFRP and GFRP strengthened members under monotonic and cyclic loadings.

Table 3: Comparison between experimental and theoretically predicted ultimate moment capacities.

Beams identification	Ultimate Moment capacity (kN.m)		$\dfrac{M_{EXP}}{M_{Theo}}$
	Theoretical (M_{Theo})	Experimental (M_{EXP})	
BB-B-M	4.76	5.30	1.11
SB-C-M	8.05	8.00	0.99
SB-G-M	7.16	7.30	1.02
BB-B-C	4.61	5.14	1.11
SB-C-C	7.00	6.96	0.99
SB-G-C	6.63	6.76	1.02
		Mean Ratio	1.04
		COV	0.05

5. Conclusions

The structural response of simply-supported bare, CFRP and GFRP strengthened CHS beams under monotonic and cyclic loading has been investigated through experimental testing. The results show that both CFRP and GFRP strengthening techniques effectively enhanced the structural performances of CHS beam under monotonic and large-displacement cyclic loadings. The resulting benefits and conclusions of CRFP and GFRP strengthening techniques are summarised as follows:

- The ultimate moment capacity of the CHS beam under monotonic loading was significantly enhanced by both CFRP and GFRP strengthening techniques, but notably, the CFRP strengthened beam shows 5.4% higher ultimate moment capacity, while the GFRP strengthened beam shows 34.1% higher rotational capacity compared to each other.

- Stiffness and ductility of CHS beam can be effectively enhanced under monotonic loading by both CFRP and GFRP strengthening, however, the CFRP strengthened beam exhibited 5.0% higher secant stiffness, whereas the GFRP strengthened beam exhibited 39.7% ductility compared to each other.

- The ultimate moment capacity of the CHS beams was significantly improved by both FRP strengthening techniques under cyclic loading. However, the GFRP strengthened beam reached its maximum moment capacity at a greater rotational level compared to the bare and CFRP strengthened beams.

- CHS beams are significantly strengthened under cyclic loading by the increased stiffness due to CFRP and GFRP strengthening. Further, the CFRP strengthened beam shown slightly higher stiffness (1.6%) and the GFRP strengthened beam experienced slightly less stiffness degradation (2.3%) in comparison to each other.

- Both FRP materials have shown to increase the energy dissipation capacity of the CHS beams. The GFRP strengthened beam, however, had a 4.6% higher energy dissipation capacity than the CFRP strengthened beam due to its higher ductility properties.

- The ultimate moment capacities in the experimental tests for the bare, CFRP and GFRP strengthened beams were consistent with predicted values through theoretical calculations with a mean ratio of 1.04 and a COV of 0.05.

The findings of this paper will be beneficial to strengthen CHS steel members in earthquake-prone structures through CFRP and GFRP strengthening techniques. Moreover, the performance of FRP strengthened full-scale simply-supported circular hollow steel members under monotonic and large-displacement cyclic loading can be investigated numerically as a future study.

Credit authorship contribution statement

T. Tafsirojjaman: Project administration; Supervision; Conceptual-ization; Methodology; Investigation; Analysis; Writing – original draft; Writing – review and editing. **Sabrina Fawzia:** Supervision; Writing – review and editing. **David P Thambiratnam:** Supervision; Writing – review and editing. **Nicholas Wirth:** Investigation; Writing – original draft; Writing – review and editing.

Data Availability Statement

The raw/processed data required to reproduce these findings cannot be shared at this time as the data also forms part of an ongoing study.

References

[1]   Feng MQ, Mita A. Vibration control of tall buildings using mega subconfiguration. Journal of Engineering Mechanics 1995;121:1082–8.

[2]   Guha-Sapir D, Below R, Hoyois P. EM-DAT: International disaster database. Catholic University of Louvain: Brussels, Belgium 2015.

[3]   Nazri FM. Prediction of The Collapse Load for Moment-Resisting Steel Frame Structure Under Earthquake Forces (Penerbit USM). Penerbit USM; 2015.

[4]   ANSI/AISC 341-16. Seismic Provisions for Structural Steel Buildings, 2016. https://doi.org/111.

[5]   Seica M v., Packer JA. FRP materials for the rehabilitation of tubular steel structures, for underwater applications. Composite Structures 2007;80:440–50. https://doi.org/10.1016/j.compstruct.2006.05.029.

[6]   Kaan BN, Alemdar F, Bennett CR, Matamoros A, Barrett-Gonzalez R, Rolfe S. Fatigue enhancement of welded details in steel bridges using CFRP overlay elements. Journal of Composites for Construction 2012;16:138–49. https://doi.org/10.1061/(ASCE)CC.1943-5614.0000249.

[7]   Parker M, Steenkamp D. The economic impact of the Canterbury earthquakes. Reserve Bank of New Zealand Bulletin 2012;75:13–25.

[8]   Tafsirojjaman T, Fawzia S, Thambiratnam D. Numerical investigation on the seismic strengthening of steel frame by using normal and high modulus CFRP. Proceedings of the seventh Asia-Pacific Conference on FRP in Structures (APFIS), International Institute for FRP in Construction (IIFC); 2019.

[9]   Liu Y, Tafsirojjaman T, Dogar AUR, Hückler A. Shrinkage behavior enhancement of infra-lightweight concrete through FRP grid reinforcement and development of their shrinkage prediction models. Construction and Building Materials 2020;258.

[10]   Liu Y, Tafsirojjaman T, Dogar AUR, Hückler A. Bond behaviour improvement between infra-lightweight and high strength concretes using FRP grid reinforcements and development of bond strength prediction models. Construction and Building Materials 2020;270:121426. https://doi.org/10.1016/j.conbuildmat.2020.121426.

[11]   Tafsirojjaman T, Fawzia S, Thambiratnam D, Zhao XL. Seismic strengthening of rigid steel frame with CFRP. Archives of Civil and Mechanical Engineering 2019;19:334–47. https://doi.org/10.1016/j.acme.2018.08.007.

[12]   Bhatt PP, Kodur VKR, Shakya AM, Alkhrdaji T. Performance of insulated FRP-strengthened concrete flexural members under fire conditions. Frontiers of Structural and Civil Engineering 2021.

[13]   ASTM E119. Standard test methods for fire tests of building construction and materials, ASTM Philadelphia; 2012.

[14]   Imran M, Mahendran M. Fire behaviour of CFRP strengthened short SHS steel columns with and without insulation. Composites Part B: Engineering 2020;193:108016. https://doi.org/10.1016/j.compositesb.2020.108016.

[15]   Tafsirojjaman T, Fawzia S, Thambiratnam DP. Investigation on the behaviour of CFRP strengthened CHS members under Monotonic loading through finite element modelling. Structures 2020;28:297–308.

[16]   Kabir MH, Fawzia S, Chan THT, Gamage JCPH, Bai JB. Experimental and numerical investigation of the behaviour of CFRP strengthened CHS beams subjected to bending. Engineering Structures 2016;113:160–73. https://doi.org/10.1016/j.engstruct.2016.01.047.

[17]   Tafsirojjaman T, Fawzia S, Thambiratnam D, Zhao XL. Behaviour of CFRP strengthened CHS members under monotonic and cyclic loading. Composite Structures 2019;220:592–601. https://doi.org/10.1016/j.compstruct.2019.04.029.

[18]   Tafsirojjaman T, Fawzia S, Thambiratnam D, Zhao X. Numerical investigation of CFRP strengthened RHS members under cyclic loading. Structures 2020;24:610–26. https://doi.org/10.1016/j.istruc.2020.01.041.

[19]   Tafsirojjaman T, Fawzia S, Thambiratnam DP, Zhao XL. Study on the cyclic bending behaviour of CFRP strengthened full-scale CHS members. Structures 2020;28:741–56. https://doi.org/10.1016/j.istruc.2020.09.015.

[20]   Kesavan K, Ravisankar K, Senthil R, Ahmed AKF. Experimental studies on performance of reinforced concrete beam strengthened with CFRP under cyclic loading using FBG array. Measurement 2013;46:3855–62.

[21]   Siwowski TW, Siwowska P. Experimental study on CFRP-strengthened steel beams 2018;149:12–21.

[22]   Tafsirojjaman T, Fawzia S, Thambiratnam D Numerical investigation on the CFRP strengthened steel frame under earthquake. 995. Materials Science Forum; 2020. p.123–9.

[23]   Tafsirojjaman, Fawzia S, Thambiratnam D. Enhancement Of Seismic Performance Of Steel Frame Through CFRP Strengthening. Procedia Manufacturing 2019;30:239–46. https://doi.org/10.1016/j.promfg.2019.02.035.

[24]   Alam MI, Fawzia S, Tafsirojjaman T, Zhao XL. FE modeling of FRP strengthened CHS members subjected to lateral impact. Tubular Structures XVI: Proceedings of the 16th International Symposium for Tubular Structures (ISTS 2017, 4-6 December 2017, Melbourne, Australia), CRC Press; 2017, p. 409.

[25]   Batuwitage C, Fawzia S, Thambiratnam DP, Tafsirojjaman T, Al-Mahaidi R, Elchalakani M. CFRP-wrapped hollow steel tubes under axial impact loading. Tubular Structures XVI: Proceedings of the 16th International Symposium for Tubular Structures (ISTS 2017, 4-6 December 2017, Melbourne, Australia), CRC Press; 2017, p. 401.

[26]   Alam MI, Fawzia S, Zhao XL, Remennikov AM, Bambach MR, Elchalakani M. Performance and dynamic behaviour of FRP strengthened CFST members subjected to lateral impact. Engineering Structures 2017;147:160–76. https://doi.org/10.1016/j.engstruct.2017.05.052.

[27]   Photiou NK, Hollaway LC, Chryssanthopoulos MK. Strengthening of an artificially degraded steel beam utilising a carbon / glass composite system 2006;20:11–21. https://doi.org/10.1016/j.conbuildmat.2005.06.043.

[28]   Accord NB, Earls CJ. Use of Fiber-Reinforced Polymer Composite Elements to Enhance Structural Steel Member Ductility. Journal of Composites for Construction 2006;10:337–44. https://doi.org/10.1061/(ASCE)1090-0268(2006)10:4(337).

[29]   Siddique MAA, El Damatty AA. Improvement of local buckling behaviour of steel beams through bonding GFRP plates. Composite Structures 2013;96:44–56. https://doi.org/10.1016/j.compstruct.2012.08.042.

[30]   Harries KA, Peck AJ, Abraham EJ. Enhancing stability of structural steel sections using FRP. Thin-Walled Structures 2009;47:1092–101. https://doi.org/10.1016/j.tws.2008.10.007.

[31]   El Damatty AA, Abushagur M, Youssef MA. Experimental and analytical investigation of steel beams rehabilitated using GFRP sheets. Steel and Composite Structures 2003;3:421–38. https://doi.org/10.12989/scs.2003.3.6.421.

[32]   Jia J, Han Q, Xu Z, Zhang D. Cyclic load responses of GFRP-strengthened hollow rectangular bridge piers. Advances in Materials Science and Engineering 2014;2014.

[33]   Attari N, Amziane S, Chemrouk M. Flexural strengthening of concrete beams using CFRP, GFRP and hybrid FRP sheets. Construction and Building Materials 2012;37:746–57. https://doi.org/10.1016/j.conbuildmat.2012.07.052.

[34]   Hamrat M, Bouziadi F, Boulekbache B, Daouadji TH, Chergui S, Labed A, et al. Experimental and numerical investigation on the deflection behavior of pre-cracked and repaired reinforced concrete beams with fiber-reinforced polymer. Construction and Building Materials 2020;249:118745.

[35]   AS 1391. Metallic materials-Tensile testing at ambient temperature, 2007.

[36]   ASTM D3039. Standard Test Method for Tensile Properties of Polymer Matrix Composite Materials, 2008.

[37]   ASTM D638. Standard Test Method for Tensile Properties of Plastics., 2010.

[38]   Tafsirojjaman T, Fawzia S, Thambiratnam DP, Zhao XL FRP strengthened SHS

beam-column connection under monotonic and large-deformation cyclic loading. Thin-Walled Structures 2021;161:107518. https://doi.org/.org/10.1016/j.tws.2021.107518.

[39]   Jiao H, Zhao XL. CFRP strengthened butt-welded very high strength (VHS) circular steel tubes. Thin-Walled Structures 2004;42:963–78. https://doi.org/10.1016/j.tws.2004.03.003.

[40]   Duarte APC, Silva BA, Silvestre N, de Brito J, Júlio E, Castro JM. Tests and design of short steel tubes filled with rubberised concrete. Engineering Structures 2016;112:274–86. https://doi.org/10.1016/j.engstruct.2016.01.018.

[41]   Li ZX. Theory and technique of engineering structure experiments. Tianjin University Press Tianjin 2004.

[42]   Haedir J, Bambach MR, Zhao XL, Grzebieta RH. Strength of circular hollow sections (CHS) tubular beams externally reinforced by carbon FRP sheets in pure bending. Thin-Walled Structures 2009;47:1136–47. https://doi.org/10.1016/j.tws.2008.10.017.

[43]   AS 4100: Steel structures, Standards Australia. 2016.